Journal of the European Ceramic Society 19 (1999) 2625–2631

PII: S0955-2219(99)00043-6
0955-2219/99/$ - see front matter

Examination of the Indentation Size Effect in Low-load Vickers Hardness Testing of Ceramics

Jianghong Gong,* Jianjun Wu and Zhenduo Guan

Department of Materials Science and Engineering, Tsinghua University, Beijing 100084, People's Republic of China

(Received 3 December 1998; accepted 6 February 1999)

Abstract

The indentation size effect (ISE) in Vickers hardness for several ceramic materials was observed in a relatively wider range of applied test load. It was shown that the proportional specimen resistance (PSR) model proposed by Li and Bradt is insufficient for describing the experimental data. By considering the effect of the machining-induced plastically deformed surface on the hardness measurements, the PSR model was modified and the empirical equation proposed originally by Bückle was proven to be more suitable for correlating the measured indentation dimension to the applied test load. © *1999 Elsevier Science Limited. All rights reserved*

Keywords: indentation size effect, hardness, mechanical properties, modelling.

1 Introduction

Indentation hardness testing is a convenient means of investigating the mechanical properties of a small volume of materials. The conventional procedure of hardness testing consists of applying a fixed load on a diamond indentor and measuring, with the help of a microscopy, the dimension of the resultant indentation on the surface of the test material after unloading. Among a variety of indentor geometries used in hardness testing, the Vickers indentor is one in most widespread use. The Vickers diamond pyramid hardness number, H_V, is defined as the ratio of the applied load, P, to the pyramidal contact area, A, of the indentation:

$$H_V = P/A = \alpha P/d^2 \tag{1}$$

*To whom correspondence should be addressed c/o Professor Zhenduo Guan. E-mail: gong@tonghua.com.cn

where d is the length of the diagonal of the resultant impression, and $\alpha = 1{\cdot}8544$ for Vickers indentor.

Investigations have confirmed that the hardness number calculated with eqn (1) is usually load-dependent.[1–5] When a very low load is used, the measured hardness is usually high; with an increase in test load, the measured hardness decreases. Such a phenomenon is sometimes referred to as *indentation size effect* (ISE). Undoubtedly, the existence of the ISE may hamper or preclude plausible hardness measurements. Furthermore, using a load-dependent hardness number in material characterization may result in some unreliable conclusions.

Much research work has been performed to explain the origin of the ISE and several possible explanations exist. These explanations fall into two sets. The first set, which is the most common explanation found in the literature, concerns the experimental errors resulting from the limitations of the resolution of the objective lens[6,7] and the sensitivity of the load cell.[8] The second set, which is described by Bückle[9] as the apparent cause of errors, is directly related to the intrinsic structural factors of the test materials, including indentation elastic recovery,[10] work hardening during indentation,[11] surface dislocation pining,[12] etc. Recent reviews[13] showed that, despite much interest, the cause of the ISE has never been satisfactorily achieved.

Recently, Li and Bradt[14] developed a proportional specimen resistance (PSR) model to explain the observed ISE in two rutile-structural single crystals, TiO_2 and SnO_2. In this model, the applied test load, P, and the resultant indentation dimension, d, are predicted to follow the relationship

$$P = a_1 d + a_2 d^2 \tag{2}$$

The observed ISE is considered to be a consequence of the indentation-size proportional resistance of the test specimen as described by a_1-term and the a_2-term can be related directly to the

load-independent hardness. The contributing factors to the proportional specimen resistance have been suggested to be the friction effect between the indentor facets and the test specimen, and the elastic resistance of the test specimen.

The aim of the present work is to investigate the load dependence of the measured Vickers hardness of some typical glasses and ceramics, with a particular emphasis on the applicability of the PSR model within a relatively wider range of applied test load.

2 Experimental

The materials chosen for this study are listed in Table 1, along with pertinent information on preparation and mechanical properties. Among these materials, the two grades of Si_3N_4, FD-02 and FD-03, and the three grades of Ti(C,N)-based cements, TCN-1, TCN-2 and TCN-3, were supplied by Found Corporation, China; the soda-lime glass was received as a commercial product; and the rest were fabricated in the laboratory.

The ceramic and cement specimens were received with machined surfaces. With these materials the machining damage was removed mechanically by polishing, ultimately with 0·5 μm diamond paste, to produce an optical finish. The glass specimen needed no such preparation, for its surface is mirror smooth as a result of the fabrication history. All specimens were in slab form with flat, parallel surfaces.

Vickers hardness measurements were made with a low-load hardness tester at load levels ranging from 5 to 50 N and at a constant indentor dwell time of 30 s. All indentation tests were carried under ambient laboratory conditions. After indentation, the length of each of the two diagonals of the square-shaped Vickers indentation was immediately measured by optical microscopy with a magnification of 300 and an error of measurement of $\pm 1\,\mu$m.

3 Results and Discussion

3.1 Indentation size effect in measured hardness

The Vickers hardness numbers, H_V, for the 12 materials listed in Table 1 were determined according to eqn (1) and are plotted in Fig. 1 as functions of the applied test load, P. Each of the data points represents an average of measurements from at least five tests. For the sake of conciseness, all the

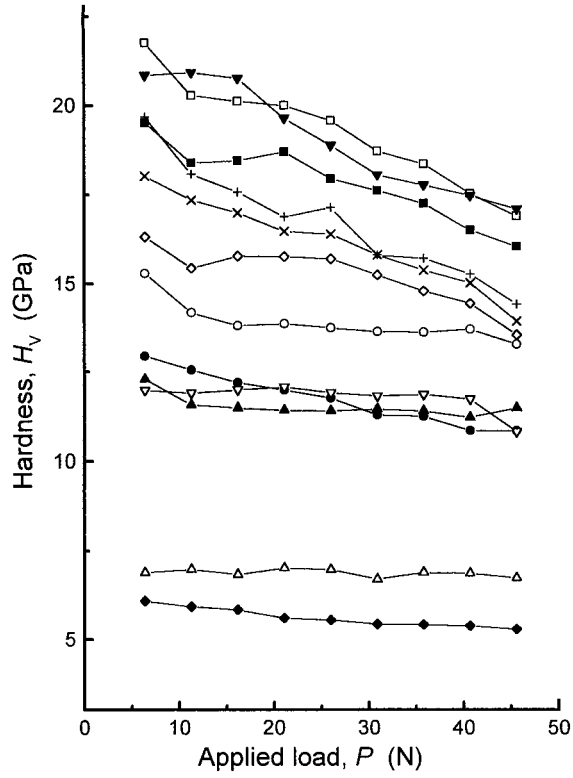

Fig. 1. Vickers hardness as functions of the applied test load for materials tested. (■) FD-02; (□) FD-03; (●) Si_3N_4/SiC_w; (○) Al_2O_3; (▲) TZP; (△) mullite; (▽) ZTM; (▼) SiC; (◆) glass; (◇) TCN-1; (+) TNC-2; (×) TCN-3.

Table 1. Specifications of materials used in this study

Material	*Preparation*	*Elastic modulus* E *(GPa)*	*Fracture toughness* K_{IC} *(MPa$\sqrt{m}$)*
Si_3N_4 (FD-02)	Hot-pressed	288	5·8[a]
Si_3N_4 (FD-03)	Hot-pressed	291	4·8[a]
Sic whisker toughened Si_3N_4 (Si_3N_4/SiC_w)	Hot-pressed	323	11·2[b]
Al_2O_3	Sintered	388	3·7[a]
ZrO_2 (TZP)	Sintered	200	10·2[a]
Mullite	Sintered	180	2.0[b]
ZrO_2 toughened mullite (ZTM)	Sintered	174	5·6[b]
SiC	Sintered	430	2·9[b]
Soda-lime glass		70	0·8[15]
Ti(C,N)-based cement (TCN-1)	Sintered		6·5[a]
Ti(C,N)-based cement (TCN-2)	Sintered		12·4[a]
Ti(C,N)-based cement (TCN-3)	Sintered		8·5[a]

[a]Measured with conventional single-edge-notched beam (SENB) method.
[b]Measured with a modified Knoop-indented bending beam method.[16]

error bars corresponding to each data point are omitted. The maximum scatter, typically 5–6% of the hardness value, usually occurs at the lower load range and is reduced as the applied load increases.

A significant ISE was observed in the materials whose apparent hardness values at 6·37 N load, denoted as $H_{6\cdot37}$, are larger than 12·5 GPa, while there is a slight decreasing tendency in the measured Vickers hardness of the materials with $H_{6\cdot37}$ values smaller than 12·5 GPa. Especially, the measured hardness for mullite was nearly independent of the applied load.

The load-dependence of the measured Vickers hardness values can also be described quantitatively through the application of the classical Meyer's law:[3,4,14]

$$P = Ad^n \tag{3}$$

where A and n are constants that can be derived directly from the curve fitting of the experimental data. Table 2 summarizes the Meyer's law parameters determined by the regression analyses of the results shown in Fig. 1. Note that the ISE is usually related to the deviation of the n-value from two, for n is equal to two in the absence of an ISE. The analysis results listed in Table 2 indicate that, among all the test materials, the most significant ISE was observed in TCN-2 ($n = 1\cdot748$) while the ISE observed in mullite ($n = 1\cdot979$) is negligible.

Bückle[9] has identified three regions of Vickers hardness testing conditions: 'microhardness' (<200 gf), 'low-load hardness' and 'normal hardness' (>2 Kgf). According to Bückle's description, only the 'low-load' condition was definitely associated with the decreasing tendency in measured hardness number as load increases. It should be pointed out, however, that the identification made by Bückle was based mainly on the available experimental data on metals and single crystals, whose hardness values are much smaller than those of brittle ceramics. In fact, as indicated in Fig. 1, the present study has shown that the ISE in ceramics may extend to much higher load. It is necessary, therefore, to explore the load-dependence of the measured hardness in ceramics over a relatively wider range of the applied test load.

Table 2. Regression analysis results of the experimental data according to Meyer's law

Material	*log A*	*n*
FD-02	3·769	1·839
FD-03	3·738	1·793
Si_3N_4/SiC_w	3·587	1·826
Al_2O_3	3·738	1·892
TZP	3·683	1·912
Mullite	3·546	1·979
ZTM	3·768	1·970
SiC	3·731	1·790
Glass	3·332	1·860
TCN-1	3·740	1·865
TCN-2	3·625	1·748
TCN-3	3·670	1·793

Due to the nature of intrinsic brittleness, Vickers indentation may result in microfracture around the impression in the surface and/or subsurface of ceramics when the applied load is high enough.[17] For all the materials tested in this study, microfracture was observed in the whole range of the applied load examined (6·37–45·57 N). Since microfracture occurs mainly during the loading, a portion of the energy, which is used to create the indentation deformation, will be dissipated by the crack formation. Thus, one can expect that, for a given material, the Vickers hardness value measured with a cracking indentation will be higher than that measured with a crack-free indentation at the same load.[18] However, it seems to be impossible to avoid the effect of microfracture on the hardness measurements in low-load range, in which the ISE is significant, for microcracking can occur in most ceramics even at loads lower than 50 gf. On the other hand, when tested below such a low load, the experimental errors related to the smallness of the indentation will be significant, sometimes making it impossible to conduct repeatable measurements.

3.2 Analysis according to the PSR model

The PSR model of Li and Bradt[14] may be considered to be a modified form of the Hays/Kendall approach to the ISE. When examining the ISE in the Knoop hardness testing of a number of metals, Hays and Kendall[19] advanced a concept that there exists a minimum level of the applied test load, W, named the test-specimen resistance, below which permanent deformation due to indentation does not initiate, but only elastic deformation occurs. They introduced an effective indentation load, $P_{eff} = P - W$, and proposed the following relationship,

$$P - W = Kd^2 \tag{4}$$

where K is a constant for a given material. Li and Bradt[14] discussed the Hays/Kendall approach and found that the measured test-specimen resistance, W, is too large to have a physical meaning. By analysing the load-indentor penetration curves measured with a variety of materials, Li and Bradt suggested that the test-specimen resistance, W, is not a constant as proposed by Hays and Kendall, but increases with the indentation size and is directly proportional to it, i.e.,[14]

$$W = a_1 d \tag{5}$$

to a first approximation, the form of eqn (5) can be considered to be similar to the elastic resistance of a spring with the opposite sign to the applied test load. Then, the effective indentation load and the indentation dimension can be related as:

$$P_{eff} = P - W = a_2 d^2 \tag{6}$$

Substituting eqn (5) into eqn (6) yields eqn (2), the relationship between the applied test load and the resultant indentation dimension, which is predicted in the PSR model.

Equation (2) can be transformed into:

$$P/d = a_1 + a_2 d \tag{7}$$

Equation (7) means that the proportional specimen resistance (PSR) described by the a_1-value and the second coefficient, a_2, can be readily evaluated through the linear regression of P/d versus d. Thus, the applicability of the PSR model to describe the observed ISE in a relatively wider range of applied test load can be examined by testing the linearity between P/d and d.

Figure 2(a) shows the $P/d - d$ curves for the three grades of Si_3N_4-based ceramics, FD-02, FD-03 and Si_3N_4/SiC_w. It is evident that, for each material, all the data points fall into two separate sets, both showing apparent linearity. For example, by fitting the experimental data for FD-02 in the lower load range according to eqn (7), a straight line with a slope of 9680 N mm^{-2} is obtained; while another straight line with a slope of 5785 N mm^{-2} is also obtained in the higher load range. Correlations for these two plots are very high, $r^2 > 0{\cdot}99$.

Similar conclusions can also be obtained by analysing the experimental data for other materials. As can be seen in Fig. 2(b)–(d), for ZTM, SiC and the three grades of Ti(C,N)-based cements, evident deviations appear when extrapolating the $P/d - d$ straight lines fitting in the lower load range to the higher load range. For Al_2O_3, TZP, mullite and soda-lime glass, however, the linear relationships between P/d and d seem to be held over the whole working range of applied test load.

It may be concluded from the above discussion that using the PSR model of Li and Bradt to explain the observed ISE in ceramics in a relatively wider range of applied test load may produce several inconsistencies. First, the PSR model describes two distinctive regimes of hardness, the indentation load-dependent, or ISE regime and the indentation load-independent regime, and eqn (2) is suggested to be valid in the ISE regime.[20] However, the experimental results show that, at least in some certain situations, the $P/d - d$ linear relationship can be observed only in a narrow range of applied test load in the explored ISE regime. Second, the

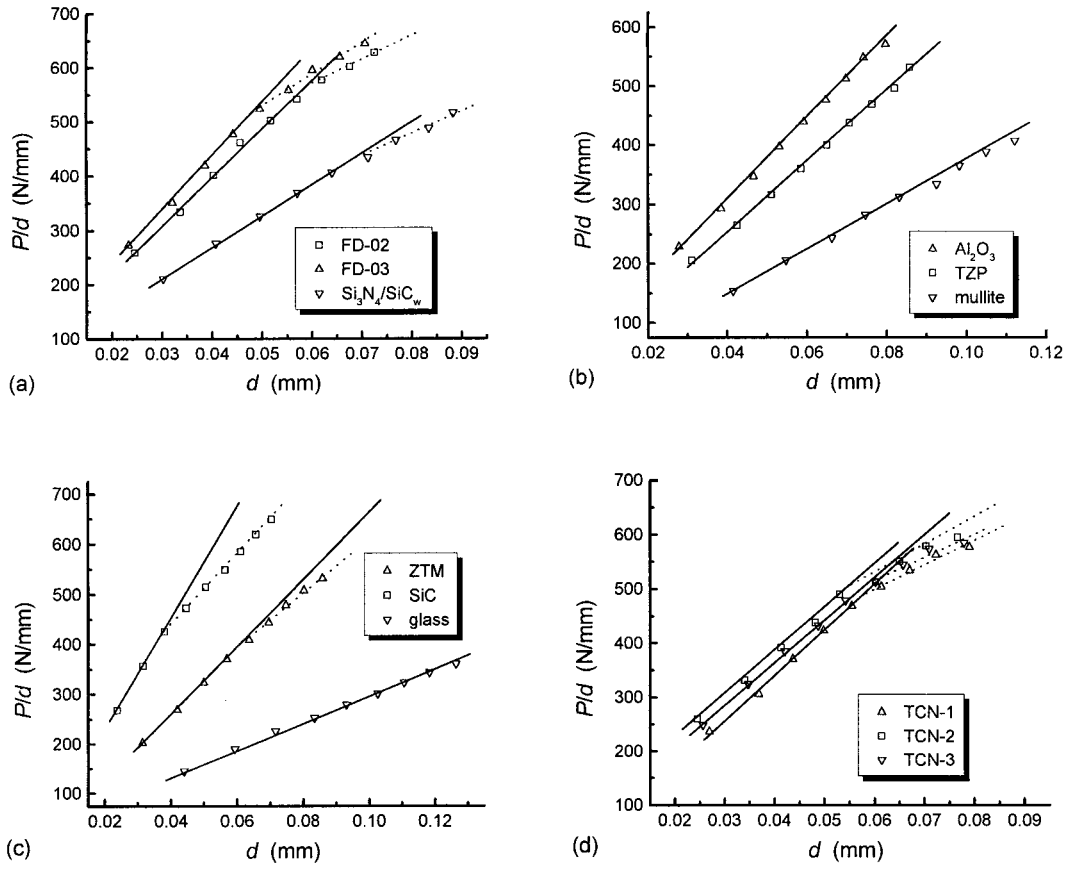

Fig. 2. P/d plotted against d for test materials.

PSR model suggests that the a_2-term in eqn (2) may be a measure of the load-independent hardness, sometimes referred to as 'true hardness'. This seems to be unreasonable, for the above discussion shows that, for some materials, different a_2-values may result if the ISE is examined in different range of applied test load, while material can not be characterized with two or more different 'true hardness' values. Thus, one can conclude that the existing PSR model does not provide a satisfactory explanation of the ISE and warrants a modification.

3.3 A modified PSR model

One possible explanation for the deviation of the $P/d - d$ relation predicted in the PSR model from the experimental results, as discussed above, is that the description of the test-specimen resistance to the permanent deformation in this model may be incorrect.

Note that, when $d = 0$, the test-specimen resistance, W, defined as eqn (5) becomes zero, implying that the minimum applied load needed to produce a plastic indentation is zero for a given material. This seems to be tenable. In fact, Li and Bradt[14] have also noted the experimental phenomenon reported by Gane and Bowder that there is a sudden indentor penetration into the surface of gold specimens at a nominal load level. For brittle ceramics, there are more reasons to believe that there is a non-zero minimum load below which permanent deformation due to indentation does not initiate. Of course, this non-zero minimum load may be very small compared with the load level used in this study and can be neglected in the calculation of the test-specimen resistance to indentation.

An important factor which may affect the test-specimen resistance of ceramics is associated with the machining and polishing, which are unavoidable, and usually the final stages, processes for the requirements of both dimensional control and surface quality control of the fine ceramic components and specimens. As described above, all the test specimens, except soda-lime glass, used in the present study were obtained with a machined and polished surface. The surface machining and polishing processes, which remove the material mechanically, may introduce both plastic deformation and cracks into the material adjacent to the surface.[21] The elastic/plastic interaction of abrasive grains with the ceramic surface has been considered analogous to a series of closely spaced, single-point indenters. As reviewed by Lawn and co-workers,[17,22] a sharp indenter plastically deforms a small volume of material. Because the plastically deformed volume elements associated with each grinding groove overlap one another, the complete surface would be plastically deformed and in a state of compression.[21] Although a quantitative analysis relating the effect of such a plastically deformed surface on the hardness measurements is still lacking, there is reason to believe that, if it is true that the material resistance of the specimen with a plastically deformed surface, W, can be simulated as the elastic resistance of a spring, such a 'spring' must have been in a state of compression, rather than stress-free, before being subjected to indentation. If this were the case, eqn (5) would be revised as:

$$W = P_0 + a_1 d \tag{8}$$

where P_0 relates to the residual surface stresses in the test specimen.

Substituting eqn (8) into eqn (6) yields:

$$P = P_0 + a_1 d + a_2 d^2 \tag{9}$$

Equation (9) can be regarded as a modified form of the existing PSR model. Thus, the physical meanings of the parameters a_1 and a_2 in eqn (9) are the same as those in eqn (2).

The applications of eqn (9) to all the materials studied in this work are now illustrated in Fig. 3. The solid lines in these plots are obtained by a conventional polynomial regression according to eqn (9). Clearly, eqn (9) is proven sufficiently suitable for the representation of the experimental data. The best-fit values of the parameters included in eqn (9) for each material are listed in Table 3. The relatively smaller, negative values of P_0 seem to be reasonable estimations of the magnitudes of the residual surface stresses for the test specimens, which have been subjected to a careful polishing after machining.

According to the analysis of Li and Bradt, a_1, and a_2 can be related to the elastic and the plastic properties of the test material, respectively. Note that material parameter E/H is a measure of the magnitude of the indentation residual stress resulting from the mismatch of the plastic zone and the surrounding elastic matrix.[23] Analogously, the a_1/a_2-value may be treated approximately as a measure of the residual stresses due to machining and polishing. Figure 4 shows the determined P_0-value as a function of the a_1/a_2-value. It is evident that there exists a strong correlation between these two parameters. This seems to be an indirect support for the above discussion.

It should be pointed out that both eqn (2), the PSR model proposed by Li and Bradt,[14] and eqn (9), the modified form of the PSR model proposed in this study, are of the same form that has been applied by Bückle[24] when utilizing a polynomial series representation of the applied indentation

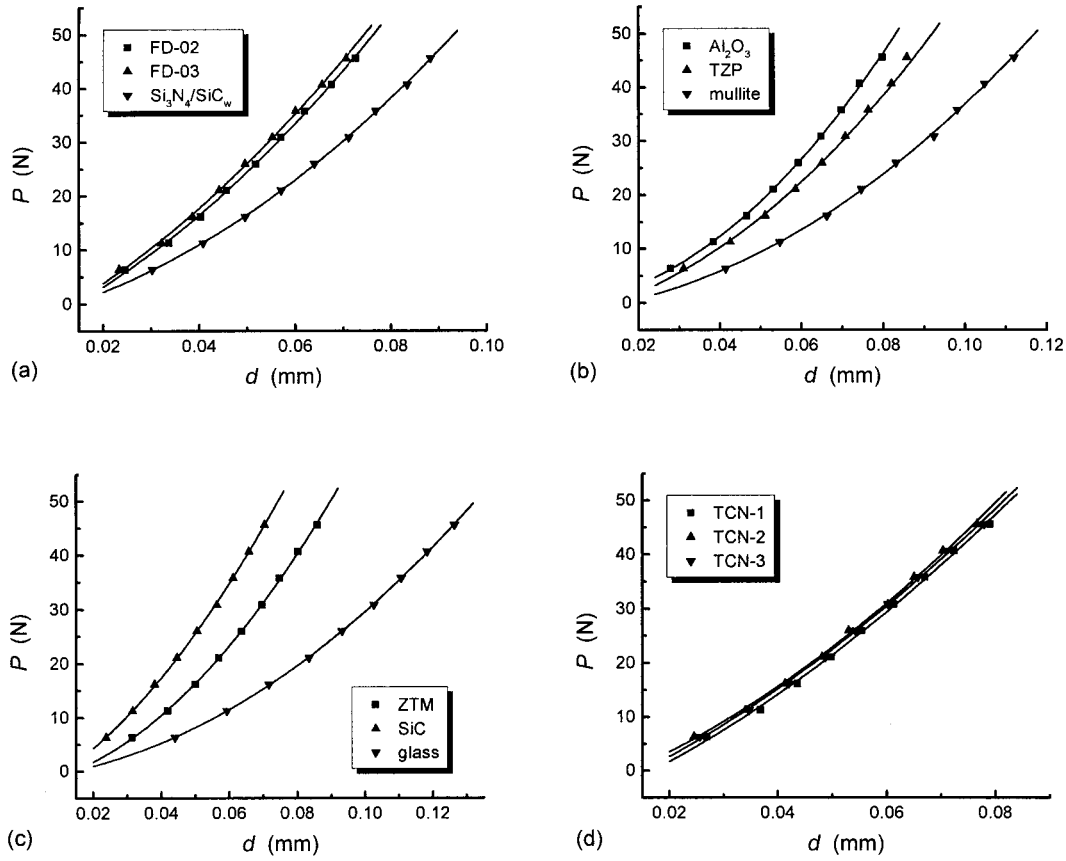

Fig. 3. Indentation size versus the applied test load for test materials.

Table 3. Regression analysis results of the experimental data according to eqn (9)

Material	P_0 *(N)*	a_1 *(N mm^{-1})*	a_2 *(N mm^{-2})*	*Correlation factor*
FD-02	−6·4	386·4	4602·9	0·9991
FD-03	−6·5	428·8	4429·9	0·9991
Si_3N_4/SiC_w	−3·3	195·0	4037·4	0·9997
Al_2O_3	−0·3	45·5	6711·0	0·9994
TZP	−2·6	128·4	4803·1	0·9989
Mullite	−1·6	56·7	3277·1	0·9993
ZTM	−2·9	126·7	5153·4	0·9997
SiC	−4·3	322·3	5490·6	0·9998
Glass	−1·5	75·1	2359·1	0·9999
TCN-1	−8·1	423·2	3375·2	0·9981
TCN-2	−5·4	366·9	4006·1	0·9986
TCN-3	−7·3	430·9	3323·2	0·9984

load to the ISE. Equation (9) differs in form from eqn (2) only in the P_0-term. In fact, many authors[25,26] as well as Li and Bradt[14] have treated P_0-term to be zero when quoting Bückle's equation, i.e. eqn (9), to describe the ISE they observed in a variety of materials. However, the findings of the present study suggest that treating P_0-term to be zero seems to be unreasonable and the original equation proposed by Bückle may provide a more satisfactory description for the observed ISE.

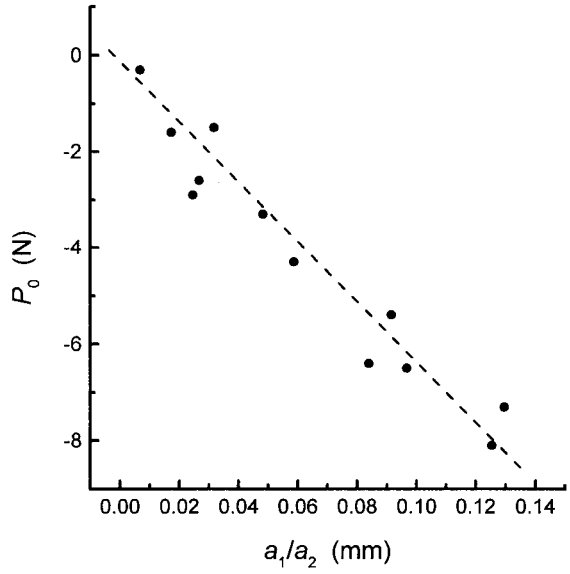

Fig. 4. Variation of P_0 with the a_1/a_2 ratio.

4 Conclusions

(a) The indentation size effect in Vickers hardness for brittle ceramics should be explored over a relatively wider range of applied test load, in order to obtain a complete understanding of this phenomenon.

(b) When being examined in a relatively wider range of applied test load, the ISE in ceramics cannot be described satisfactorily with the proportional specimen resistance model proposed by Li and Bradt.
(c) A modified PSR model was proposed by considering the effect of the machining-induced plastically deformed surface on hardness measurements.

References

1. Chakraborty, D. and Mukerji, J., Characterization of silicon nitride single crystals and polycrystalline reaction sintered silicon nitride by microhardness measurements. *J. Mater. Sci.*, 1980, **15**, 3051–3056.
2. Hirao, K. and Tomozawa, M., Microhardness of SiO_2 glass in various environments. *J. Am. Ceram. Soc.*, 1987, **70**, 497–502.
3. Babini, G. N., Bellosi, A. and Galassi, C., Characterization of hot-pressed silicon nitride based materials by microhardness measurements. *J. Mater. Sci.*, 1987, **22**, 1687–1693.
4. Mokhopadhyay, A. K., Datta, S. K. and Chakraborty, D., On the microhardness of silicon nitride and sialon ceramics. *J. Eur. Ceram. Soc.*, 1990, **6**, 303–311.
5. Quinn, J. B. and Quinn, G. D., Indentation brittle of ceramics: a fresh approach. *J. Mater. Sci.*, 1997, **32**, 4331–4346.
6. Brown, A. R. G. and Ineson, E., Experimental survey of low-load hardness testing instruments. *J. Iron & Steel Institute*, 1951, **169**, 376–388.
7. Bückle, I. H., Progress in micro-indentation hardness testing. *Metall. Rev.*, 1959, **4**, 49–100.
8. Mason, W., Johnson, P. F. and Varner, J. R., Importance of load cell sensitivity in determination of the load dependence of hardness in recording microhardness tests. *J. Mater. Sci.*, 1991, **26**, 6576–6580.
9. Bückle, I. H., Use of the hardness test to determine other material properties. In *The Science of Hardness Testing and its Research Application*, ed. J. H. Westbrook and H. Conrad. American Society for Metals, Metal Park, OH, 1973, pp. 453–494.
10. Tarkanian, M. L., Neumann, J. P. and Raymond, L., Determination of the temperature dependence of {100} and {112} slip in tungsten from Knoop hardness measurements. In *The Science of Hardness Testing and Its Research Application*, ed. J. H. Westbrook and H. Conrad. American Society for Metals, Metal Park, OH, 1973, pp. 187–198.
11. Mott, B. W., *Micro-Indentation Hardness Testing*. Butterworths Scientific, London, 1956.
12. O'Neill, H., *The Hardness of Metals and Its Measurement*. Sherwood, Cleveland, OH, 1934.
13. Blau, P. J. and Lawn, B. R. (eds), *Microindentation Techniques in Materials Science and Engineering*. American Society for Testing and Materials, Philadelphia, PA, 1986.
14. Li, H. and Bradt, R. C., The microhardness indentation load/size effect in rutile and cassiterite single crystals. *J. Mater. Sci.*, 1993, **28**, 917–926.
15. Anstis, G. R., Chantikul, P., Lawn, B. R. and Marshall, D. B., A critical evaluation of indentation techniques for measuring fracture toughness: I, direct crack measurements. *J. Am. Ceram. Soc.*, 1981, **64**, 533–538.
16. Gong, J. and Guan, Z., Strength/crack size relationship for Knoop indented bending specimens and its application to silicon nitride ceramic. *J. Eur. Ceram. Soc.*, 1998, **18**, 891–899.
17. Lawn, B. R. and Wilshaw, T. R., Indentation fracture: principles and applications. *J. Mater. Sci.*, 1975, **10**, 1049–1081.
18. Li, Z., Ghosh, A., Kobayashi, A. S. and Bradt, R. C., Indentation fracture toughness of sintered silicon carbide in the Palmqvist crack regimes. *J. Am. Ceram. Soc.*, 1989, **72**, 904–911.
19. Hays, C. and Kendall, E. G., An analysis of Knoop microhardness. *Metall.*, 1973, **6**, 275–282.
20. Li, H., Han, Y. H. and Bradt R. C., Knoop microhardness of single crystal sulphur. *J. Mater. Sci.*, 1994, **29**, 5641–5645.
21. Samuel, R., Chandrasekar, S., Farris, T. N. and Licht, R. H., Effect of residual stresses on the fracture strength of ground ceramics. *J. Am. Ceram. Soc.*, 1989, **72**, 1960–1966.
22. Lawn, B. R. and Marshall, D. B., Indentation fracture and strength degradation in ceramics. In *Fracture Mechanics of Ceramics* 3, ed. R. C. Bradt, D. P. H. Hasselman and F. F. Lange. Plenum, New York, 1978, pp. 205–230.
23. Lawn, B. R., Evans, A. G. and Marshall, D. B., Elastic/plastic indentation damage in ceramics: the median/radial crack system. *J. Am. Ceram. Soc.*, 1980, **63**, 574–581.
24. Bückle, H., *Mikrohärteprüfung*. Berliner Union Verlag, Stuttgart, 1965.
25. Fröhlich, F., Grau, P. and Wrellmann, W., Performance and analysis of recording microhardness tests. *Physics Status Sodili*, 1977, **42**, 79–89.
26. Michels, B. D. and Frischa, G. H., Microhardness of chalcogenide glasses of the system Se-Ge-As. *J. Mater. Sci.*, 1982, **17**, 329–334.